

To be submitted to
Nuclear Instr. and Meth.

COMITATO NAZIONALE PER L'ENERGIA NUCLEARE
Laboratori Nazionali di Frascati

LNF-74/30(P)
4 Giugno 1974

R. Andreani and A. Cattoni: POSITRON CONVERTER FOR
FRASCATI LINEAR ACCELERATOR.

LNF-74/30(P)
4 Giugno 1974

R. Andreani and A. Cattoni : POSITRON CONVERTER FOR FRASCATI LINEAR ACCELERATOR. -

Conversion of an electron beam to a positron beam is obtained at the end of the first four accelerating guides of Frascati linac, using an electron current of 200 mA peak, at 85 MeV, having a pulse width of 4 μ sec and a repetition rate variable between 3 and 250 pps.

Two different fixed targets have been designed : a high average power target used to produce a high duty cycle, 4 μ sec, 250 pps, positron beam for nuclear physics experiments, and a high positron production efficiency, low average power target, used for injection of positrons in to the storage ring. Adone, when a beam repetition rate of only 3 pps is allowed, but a high positron yield is required, to reduce the ring filling time.

1. - HIGH DUTY CYCLE TARGET. -

The high duty cycle target is made of a cylinder of OFHC copper, 13 mm thick. This is a little less than one radiation length, 13.4 mm, due to space limitation in the present optical system which has already performed very satisfactorily. Besides, according to the Crawford and Messel tables⁽¹⁾, the highest positron yield at low energies, lower than 20 MeV, with a primary electron energy between 50 and 100 MeV, should occur for a target thickness between 0.5 and 1 r.l.

Circumferential fins are accommodated on the cylinder to obtain sufficient heat transmission surface to the cooling water (see Fig. 1). Electron beam diameter on the target has to be limited to a minimum of 2 mm, to avoid damaging the target under pulse thermal stresses.

1.1. - Conversion efficiency. -

Let us compare the efficiencies of targets made of copper and tungsten, the two materials that, as we will see later, are the best

2.

choice to solve our problems.

Haissinsky⁽²⁾ computed, using the Crawford and Messel tables, the radial dependence of the emittance for the positrons emitted from the target (fig. 2 of the ref. above) under the following assumptions : point like primary electron beam, target thickness corresponding to the maximum positron yield at the electron energy considered, between 200 and 1000 MeV, positron energy between 10 and 20 MeV, target thickness between 1.5 and 3 r.l. The curve on fig. 2 of the cited report shows that 50% of the positrons are emitted within a radius of 0.16 r.l. and 75% within a radius of 0.32 r.l.

The positron matching and focusing system of the Frascati linac has already been described in detail^(3,4). Briefly, it is made of a short intense solenoidal magnetic field, B_1 , acting as a matching lens, followed by a long solenoidal field, B_2 , all along the high energy accelerating guides, with the target immersed in the field B_1 .

The positron source density does not depend, at first approximation, on the source size. It can be expressed as⁽⁵⁾:

$$(1) \quad n_c = \frac{dn}{dE d\Omega} \quad (e^+/\text{ster} \times \text{MeV}),$$

with $n_c = \text{const}$ for angles smaller than ≈ 0.2 rad and energies in the order of few tens MeV.

Considering the geometrical acceptance of the system, the positron current accelerated to the end of the linac, over the entire energy spectrum, can be evaluated as :

$$(2) \quad I_+ = n_c \Delta E \Omega ,$$

with

$$(3) \quad \Delta E \Omega = \frac{\pi^2}{2} \frac{R^2}{L_m} m_0 c^2 \frac{e B_2}{m_0 c} \left[\frac{B_2}{B_1} - \frac{R}{\rho} \right]$$

where :

L_m length of the matching lens, about 6.5 cm;

R iris useful radius in the accelerating guides;

ρ source radius.

Amman⁽⁵⁾ obtained this equation integrating over a band of energies from $0.5 E_c$ to ∞ where E_c is the positron emission energy for which the matching system is designed, corresponding to the value of the field B_1 .

As L_m cannot be modified in our case, we see that, increasing ρ , if one keeps B_2 constant, which is certainly convenient, and B_1 constant, the accelerated current decreases with ρ . Decreasing B_1 , one

can compensate for part of this, accounting for the fact that the center energy E_C will decrease and the energy spectrum of the positron beam will broaden due to larger dephasing of the particles in the lens and to bunching problems in the first high energy guide.

In the case of tungsten and copper, for which the radiation lengths are:

$$\begin{array}{ll} x_0 = 13.4 \text{ mm} & \text{copper} \\ x_0 = 3.6 \text{ mm} & \text{tungsten} \end{array}$$

the 75% radii: $\rho = 0.32 x_0$, are:

$$\rho_{\text{cu}} = 4.3 \text{ mm} ; \quad \rho_{\text{w}} = 1.15 \text{ mm} ,$$

keeping B_1 , B_2 constant, which should be the worst case, we would have the efficiency reduced by a factor 3.75.

Decreasing B_1 should help and, in effect, measurements taken using test targets made by tungsten and copper, installed on the Frascati linac, have shown the reduction factor to be between 2.2 and 2.5⁽⁶⁾.

Other materials than copper could give a better efficiency but the choice of copper has been dictated by its good thermal properties as reported later.

1.2. - Thermal behaviour. -

To evaluate the thermal behaviour of the targets, we will consider the volume of material interested by the beam produced electromagnetic shower. The incident electron beam has generally a distribution at cylindrical symmetry around the beam centerline and we will designate with ρ_1 : the 75% radius, i.e. 75% of the beam current flows through a circle of radius ρ_1 . Following Haissinsky, the radial distribution of the emitted positrons, for a point like electron beam, has a 75% radius: $\rho_2 = 0.32 r.l.$ Consequently, considering that both distributions are not far from gaussians, we will assume that the positron beam, produced by a finite cross section electron beam, has a 75% radius given by:

$$(4) \quad \rho_T = \sqrt{\rho_1^2 + \rho_2^2} .$$

We assume the volume interested by the power lost by the beam, to be a cone of base radii ρ_1 and ρ_T , equivalent to a cylinder of radius:

$$(5) \quad r_1 = \frac{\rho_1 + \rho_T}{2} .$$

Pulse and average temperature rises are given by the following formulae:

4.

las :

$$(6) \quad \Delta t_{\text{pulse}} = \frac{I_{\text{peak}} \times \tau \times 2 \times 10^6}{4.18 \times \pi \times r_1^2 \times c_{\text{sp}}} \quad (\text{°C})$$

$$(7) \quad \Delta t_{\text{ave}} = \frac{I_{\text{ave}} \times \Delta E}{4.18 \times c} \quad (\text{°C})$$

with ΔE energy lost by the beam in the target:

$$(8) \quad \Delta E = 2 \times I \times \delta \times 10^6 \quad (\text{eV})$$

where :

I_{peak}	peak electron beam current	(A)
I_{ave}	average electron beam current	(A)
τ	beam pulse width	(sec)
c_{sp}	specific heat of the target material	(cal/gr °C)
δ	mass density of the target	(gr/cm ³)
l	target thickness material	(cm)
c	thermal conductance from the heat source to the water.	

Formulas (6) and (7) have been obtained under the following hypothesis and assumptions :

- a) Heat accumulation during the beam pulse ;
- b) Complete removal of the beam delivered power from the target thru the water, under steady state conditions ;
- c) Power delivered to the target by the electron beam has been calculated assuming an energy loss of 2 MeV/gr/cm².

$$(9) \quad c = \frac{\gamma \times 2\pi l}{0.5 + \ln \frac{r_2}{r_1}} \quad (\text{cal/sec}),$$

γ	thermal conductivity of the target material	(cal/cm °C sec)
r_2	target radius (see Fig. 1)	(cm).

Table I presents values of the parameters which are of concern for our calculations, for different suitable materials.

Through considerations of the different materials whose parameter values are indicated in Table I, we have decided to use copper which

presents simultaneously: a very good thermal conductivity, which limits the average temperature rise, a high specific heat which limits the pulse temperature and a reasonably high melting point.

TABLE I

	Cu	W	Ti	Mo	Au	Pt
δ mass density (gr/cm ³)	8.93	19.1	4.87	10	19.25	21.4
γ thermal conductivity (cal/cm °C sec)	0.9	0.35	0.041	0.32	0.715	0.167
c_{sp} specific heat (cal/gr °C)	0.093	0.047- -0.036	0.126	0.062	0.031	0.032
t melting point (°C)	1083	3370	1690	2600	1063	1760
radiation length (gr/cm ²)	12.85	6.9			6.9	6

Introducing in equations (6), (7), (8) and (9) the following data:

$$r_1 = 0.25 \text{ cm}, \quad r_2 = 0.5 \text{ cm} \quad (\rho_1 = 0.1 \text{ cm});$$

$$l = 1.3 \text{ cm}; \quad \tau = 4 \mu\text{sec}; \quad I_{ave} = 200 \times 10^{-6} \text{ A}; \quad I_{peak} = 0.2 \text{ A}$$

for the copper target we get:

$$\Delta t_{pulse} = 20.5 \text{ °C}; \quad \Delta t_{ave} = 180 \text{ °C}.$$

Therefore:

$$\Delta t_{max} = \Delta t_{ave} + \Delta t_{pulse} \cong 200 \text{ °C}.$$

The average power dissipated in the target is:

$$(10) \quad P_{ave} = I_{ave} \times 2 \times l \times \delta \times 10^6 \quad (\text{W})$$

and is:

$$P_{ave} = 4.65 \text{ kW}$$

at full duty.

6.

1.3. - Water cooling. -

Water flow required, assuming a water temperature rise of 20°C

$$Q = 3.5 \text{ lt/min.}$$

Cooling fins surface required, assuming the convection coefficient of heat transfer to the water to be of the order of $H = 50 \text{ W/cm}^2$

$$S = \frac{P_{\text{ave}}}{H} = 100 \text{ cm}^2.$$

The external diameter of the three circumferential fins comes out to be approx. 4.8 cm.

A model of the target, at full scale, has been built and the thermal exchange from copper to water has been tested using a welding machine delivering 6 kW to the copper disc. The power removed thru the water flow has been measured using a thermocouple setup connected to a calibrated millivoltmeter. No overheating or instabilities in the heat transmission were observed.

1.4. - Mechanical stresses in the target. -

Mechanical stresses in the target have been considered to originate from two different sources : the nonuniform radial distribution of the average temperature in the target body, and the peak temperature rise in the shower region. The superposition of these two stress distributions determines the mechanical design of the target.

1.4.1. - Steady state thermal stresses. -

We will use the stress strain relations in the form suitable for thermal stress analysis. With the constants E , ν and α denoting respectively the elastic modulus, Poisson's ratio and thermal expansion coefficient, these relations are :

$$(11) \quad \begin{aligned} \epsilon_r &= \frac{1}{E} (\sigma_r - \nu \sigma_t + E \alpha T) \\ \epsilon_t &= \frac{1}{E} (\sigma_t - \nu \sigma_r + E \alpha T) \end{aligned}$$

expressed in a cylindrical coordinates system, with the z axis located along the beam centerline. T is the temperature.

Writing the stress equilibrium relation :

$$(12) \quad \frac{d(\sigma_r)}{dr} = \sigma_t;$$

and expressing the strain components, as a function of the radial displa

cement u :

$$(13) \quad \epsilon_r = \frac{du}{dr} ; \quad \epsilon_t = \frac{u}{r} ;$$

we solve the preceding equations for the displacement u and we obtain :

$$(14) \quad \frac{d^2u}{dr^2} + \frac{1}{r} \frac{du}{dr} - \frac{u}{r^2} = \alpha(1+\nu) \frac{dT}{dr} ;$$

whose solution is :

$$(15) \quad u(r) = \frac{1}{r}(1+\nu) \int_0^r \alpha Tr dr + C_1 r + \frac{C_2}{r} ,$$

Solving eq. (11) for σ_r , σ_t and using eq. (13) and (15), we get :

$$(16) \quad \begin{aligned} \sigma_r &= \frac{E}{1-\nu^2} \left[C_1(1+\nu) - \frac{C_2}{r^2}(1-\nu) - \frac{1-\nu^2}{r^2} \int_0^r \alpha Tr dr \right] \\ \sigma_t &= \frac{E}{1-\nu^2} \left[C_1(1+\nu) + \frac{C_2}{r^2}(1-\nu) + \frac{1-\nu^2}{r^2} \int_0^r \alpha Tr dr \right] - E\alpha T ; \end{aligned}$$

where C_1 , C_2 are constants to be determined applying the appropriate boundary conditions.

These equations, applied to the problem under consideration and computed, give the following results :

At $r = 0$

$$\sigma_r = -12.7 \text{ kg/mm}^2 \quad \sigma_t = -12.7 \text{ kg/mm}^2 ;$$

where the minus sign indicates compression.

At $r = r_2$

$$\sigma_t = 12.8 \text{ kg/mm}^2 .$$

For copper :

$$E = 12.000 \text{ kg/mm}^2$$

$$\alpha = 1.7 \times 10^{-5} {}^\circ\text{C}^{-1}$$

$$\nu = 0.3 .$$

8.

1.4.2. - Pulse thermal stresses. -

The stresses due to the pulse temperature rise are given by :

at $r = r_1$

$$(17) \quad \sigma_r = \sigma_t = - E \alpha \Delta T_{\text{pulse}}$$

instantaneous value.

Replacing in the preceding equation : $\Delta T_{\text{pulse}} = 20.5^{\circ}\text{C}$ we obtain :

$$\sigma_r = \sigma_t = - 4.2 \text{ kg/mm}^2.$$

It is useful to point out that this value is obtained assuming that 100% of the heat delivered by the beam is developed in a cylinder of radius r_1 , averaged between the 75% radii of the beam current distributions of the incoming electron beam and of the outgoing positron beam. This is a very rough assumption indeed, because the volume interested by the shower is in effect a cone and also because the temperature distribution will never have discontinuities.

Considering the electrons entrance point which presumably will be the most stressed location in the target, the radius to be considered will be ρ_1 , 0.1 cm in our case, but the beam current through the circle of radius ρ_1 is only 75% of the total, according to our initial assumption. The peak temperature would then be 96°C and the pulse stress would be $- 19.5 \text{ kg/mm}^2$.

Considering the figures obtained, the situation might present some risk, from the point of view of thermal fatigue. 10 hours of operation at 250 pps correspond to 9×10^6 cycles. A true answer will be obtained only through a thorough test of the target under beam.

2. - LOW DUTY CYCLE TARGET. -

This target is made of pure tungsten, 1.1 r.l. thick. Target layout is represented in Fig. 1. Water cooling is brought close to the beam centerline in a copper jacket. Six operational positions are available, to avoid the need to replace the entire target in case of punch through of the material in one of them.

2.1. - Thermal behaviour. -

2.1.1. - Pulse temperature rise. -

Using formula (6), with the following parameter values :

$$I_{\text{peak}} = 0.2 \text{ A} \quad \rho_1 = 0.05 \text{ cm}$$

$$\tau = 4 \mu\text{sec}$$

$r_1 = 0.0825 \text{ cm}$ average shower radius

$c_{sp} = 0.036 \text{ cal/gr } ^\circ\text{C}$ between 0°C and 1000°C

we obtain

$$\Delta t_{pulse} = 515^\circ\text{C},$$

averaged along the target thickness, with a maximum of 1010°C , at the entrance point of the electron beam in the target, again considering 75% of the beam current within radius r_1 .

2.1.2. - Average temperature rise.-

Using formulas (7) and (8): $\Delta E = 15.3 \text{ MeV}$ (this figure has been checked experimentally, see ref. (6)), and Δt_{ave} has been expressed as:

$$\Delta t_{ave} = \frac{I_{peak} \times \tau \times f_r \times \Delta E}{4.18 \times C} \quad (\text{°C})$$

with: f_r beam repetition frequency pulses/sec.

C has been evaluated, for the considered target layout (Fig. 1), through a graphical analysis and results $C = 0.29 \text{ cal/sec } ^\circ\text{C}$, for the worst case operational position.

Therefore :

$$\Delta t_{ave} = 10.3 f_r \quad (\text{°C}).$$

At a repetition frequency of 3 pulses/sec, which is consistent with the use of the linac as injector for the storage ring, total average temperature rise between water and target centerline is :

$$\Delta t_{ave} = 31^\circ\text{C}.$$

This target then could probably be used also at 50 pulses/sec, from the thermal point of view.

2.2. - Mechanical stresses in the target. -

Steady state thermal stresses are very low, due to the low t_{ave} in the target and will not be of concern.

Under pulse conditions, neglecting the contribution of the copper ring surrounding the tungsten plate, using expression (17) with $E = 37000 \text{ kg/mm}^2$; $\alpha = 4.6 \times 10^{-6} \text{ } ^\circ\text{C}^{-1}$ we have :

$$\text{at } r = r_1$$

$$\sigma_r = \sigma_t = - 88 \text{ kg/mm}^2,$$

10.

averaged along the target thickness, with a peak instantaneous of - 174 kg/mm², for σ_r and σ_t , at the beam entrance point.

These stresses are to be compared with the tensile strength of tungsten at ambient temperature, which, for hard drawn material, is between 250 and 400 kg/mm². The region outside the shower region is in fact at ambient temperature during the heat deposition. In time, the heat will be transmitted to the cooling water and the outer material will warm up, but the stresses will also drop because the overtemperature gradient will decay.

Mechanical behaviour of tungsten under these cycling conditions is not known. A similar target, under the same loading conditions but with a worse cooling, has experienced about 10^6 pulses without any significant damage (except a small pit few tenths of a mm wide and deep, at the beam entrance point) $\Phi \sim 0.3$ mm, ~ 0.2 mm deep.

3. - POSITRON CONVERTER. -

3.1. - Mechanical layout. -

Fig. 2 reports a picture of one of the three complete conversion systems which have been built, and Fig. 3 shows a drawing of the positron lens with the positron converter installed. Main concern, in the mechanical design, has been to achieve as high an operational reliability as possible and to make easy installing and disassembling the unit. This is related to the extremely high induced radiation level of the positron lens and to the fact that the target will also build up a very high radioactivity, after a few hours of operation at full duty.

Consequently, the entire procedure to be followed to install or to disassemble the unit has been studied to allow the operator to remotely control the different operations to be performed. In particular, during the installation, the target support chassis can be lowered on the positron lens or removed, guided by two columns, using a remotely operated crane. The vacuum tightness of the housing is made, by means of an indium gasket, through a flange, on the chassis, which is forced against the opposite flange on the housing by a motor.

3.2. - Converter controls. -

As we already said, and as indicated in Fig. 1, there are seven possible operating positions of the target, in the positron mode of operation, six with tungsten and one with copper on the beam centerline. The six tungsten positions will be used to produce positron beams for injection in the storage ring. The copper target will be used to produce high duty cycle positron beams for experiments with monochromatic gamma rays, in the LEALE area. The operator in the control room can

choose anyone of the positions of the target he wants. Compatibility with the type of run to be performed, high duty or low duty, is ensured through interlocking.

Besides the controls related to the positron lens, the following parameters are continuously monitored on the control console: cooling water flow thru the target, water temperature difference between input and output and power delivered to the target by the beam. Adjustable trips allow the operator to ensure an automatic halt of the operation in case of anomalous values assumed by the parameters.

3.3. - Converter operation. -

One of the three conversion systems built has been installed on the linear accelerator during March, 1971 and since then it has been performing satisfactorily. The only exception was a single failure of the copper target which was punched through, due to incorrect operation of the electron beam whose diameter on the target was found to be less than 0.5 mm. The repair operation (half a day totally) demonstrated the correct design of the conversion system even from the point of view of easiness of remote handling.

Total number of pulses on the copper target has been approximately 1.3 millions up to now under the following electron beam typical operating conditions :

- electron beam current: 200 - 250 mA, 50 % modulated;
- beam diameter on the target: \approx 2 mm;
- beam repetition frequency: 150 pps maximum.

Operation with 200 mA, 150 pps electron beam, unmodulated, has given a measured power deposition of : 2.6 kW against 2.8 kW theoretical, calculated from formula (10).

Total number of pulses on the tungsten target has been over many millions with the same electron beam parameters.

The comparison between the conversion efficiencies of the copper and tungsten targets has given the following results : using the same current of electron beam: 220 mA, with the same focussing conditions : \approx 2 mm beam diameter on the target, and optimizing the value of B_1 (see par. 1.1), the maximum positron currents obtained at the end of the linac are respectively :

copper target:	170 μ A peak on the 4 μ sec pulse flattop;
tungsten target:	280 μ A " " " " "

The ratio between the two conversion efficiencies results therefore approximately: 1.6. This low value depends mainly from the quite large size of the electron beam on the target.

ACKNOWLEDGMENTS. -

The authors wish to thank Prof. F. Amman for many helpful suggestions and for spending considerable time in technical discussions on the project.

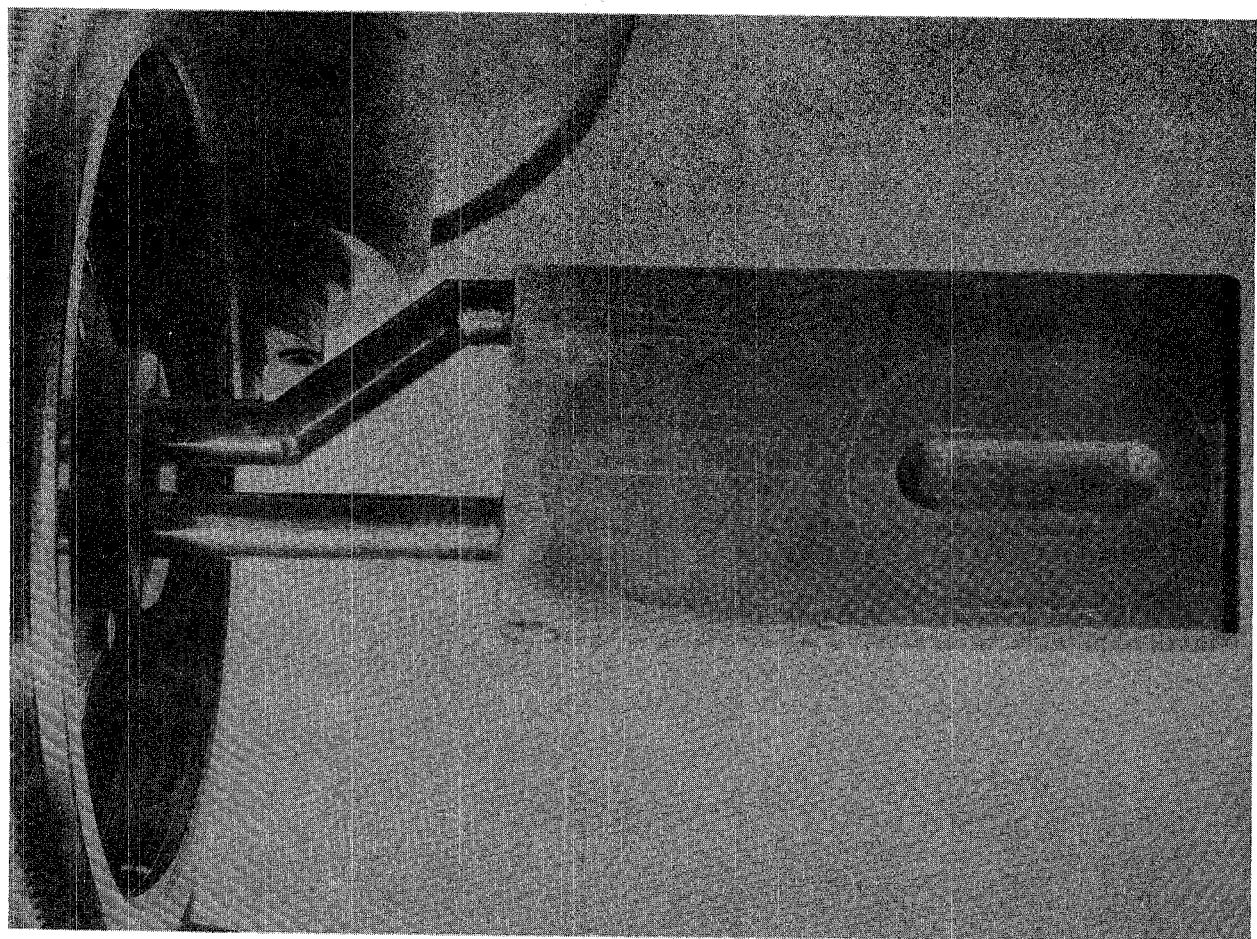
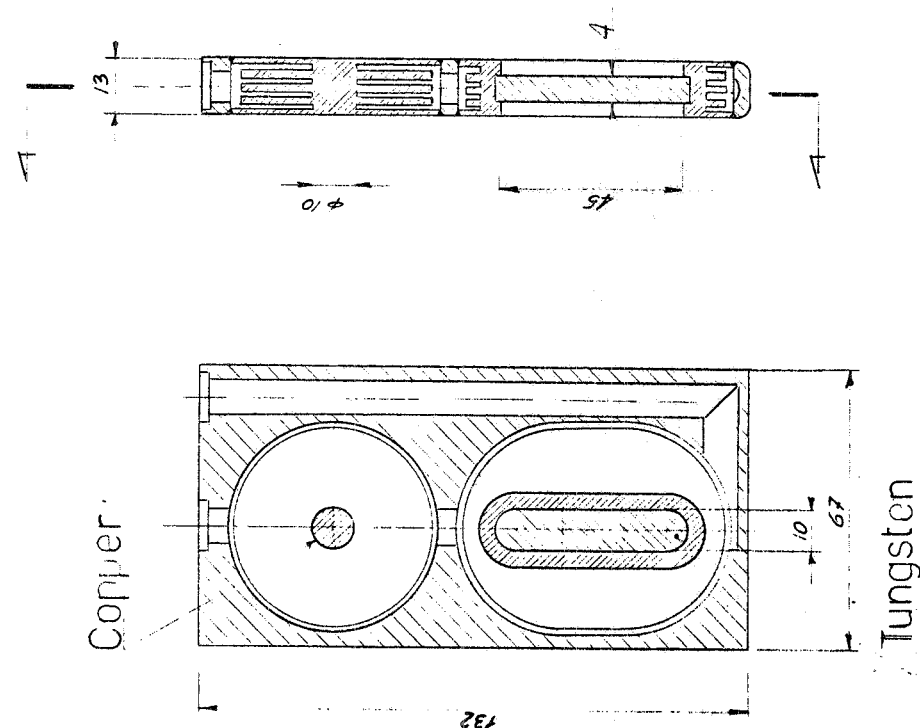
In many aspects of the converter design and construction, of great help has been the experience and the enthusiastic support of many people working at the National Frascati Laboratories. In particular, the authors are greatly indebted to Mr. Dulach for many parts of the mechanical design, to Mr. Vitali and Guiducci, who have built, in spite of many problems, an excellent target body and to Mr. Borghini, Coleschi and D'Armini who largely cooperated in the design and breadboarding of all the control system.

To all the persons here mentioned and to all the others involved, the authors wish to express their deep gratitude.

REFERENCES. -

- (1) - D.F. Crawford and H. Messel, The electron-photon cascade in lead, emulsion and copper absorbers, Nuclear Phys. 61, 145 (1965).
- (2) - J. Haissinsky, Faisceau de positrons pour l'anneau de collision ACO, Orsay rapport technique 25-65 (1965).
- (3) - F. Amman e R. Andreani, L'acceleratore lineare per elettroni e positroni, Frascati report LNF-63/46 (1963).
- (4) - C. Nunan, A positron linear accelerator design, IEEE Trans. on Nuclear Sci. NS-12, 465 (1965).
- (5) - P. M. Lapostolle and A. L. Septier, Linear accelerators (North Holland, 1970).
- (6) - R. Andreani e A. Cattoni, Misure di perdita di energia e di rendimento di conversione elettroni-positroni, in targhette di rame e di tungsteno, Progetto Adone - memorandum interno L 4 (1970).

FIG. 1 - Target



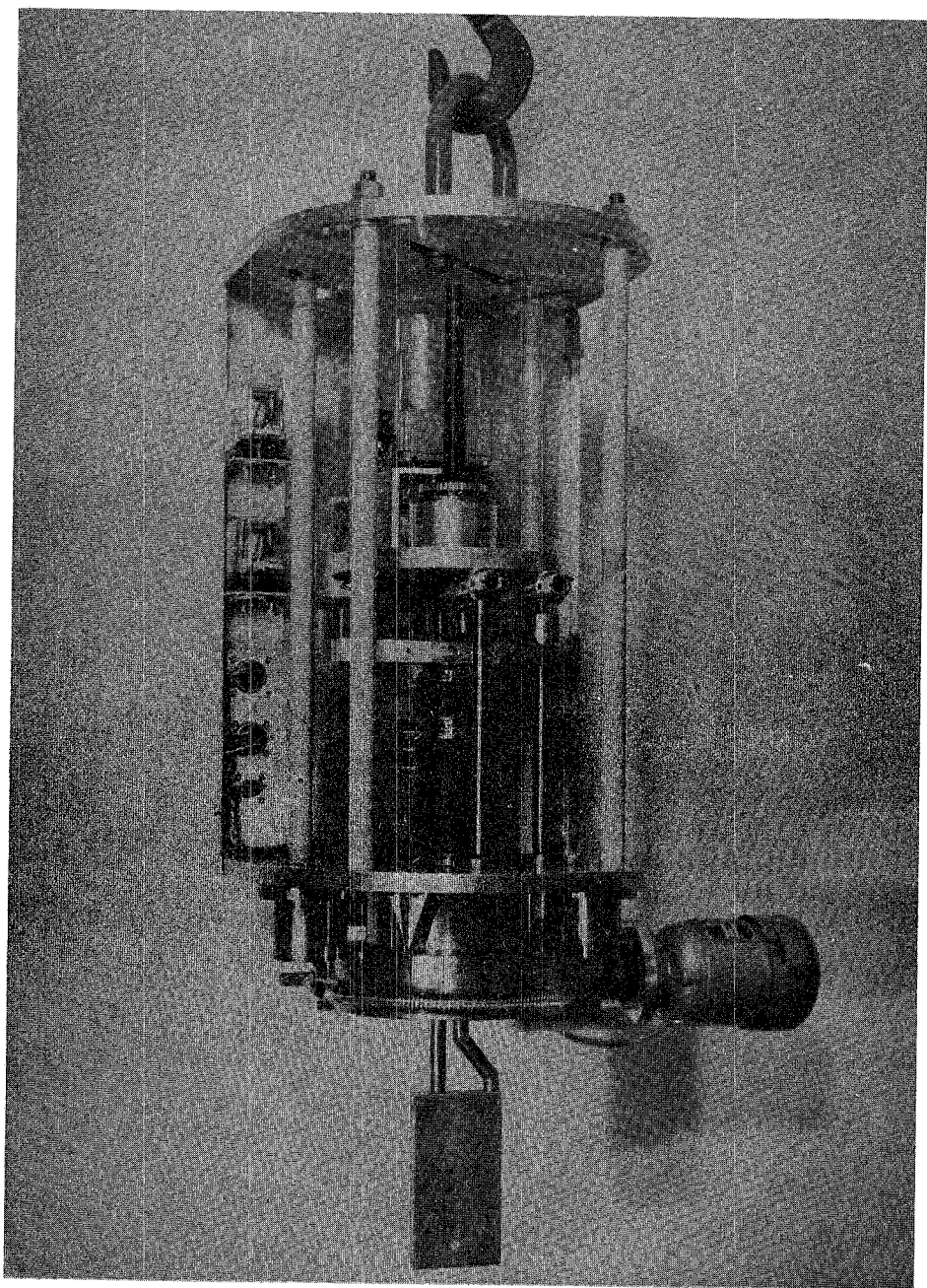


FIG. 2

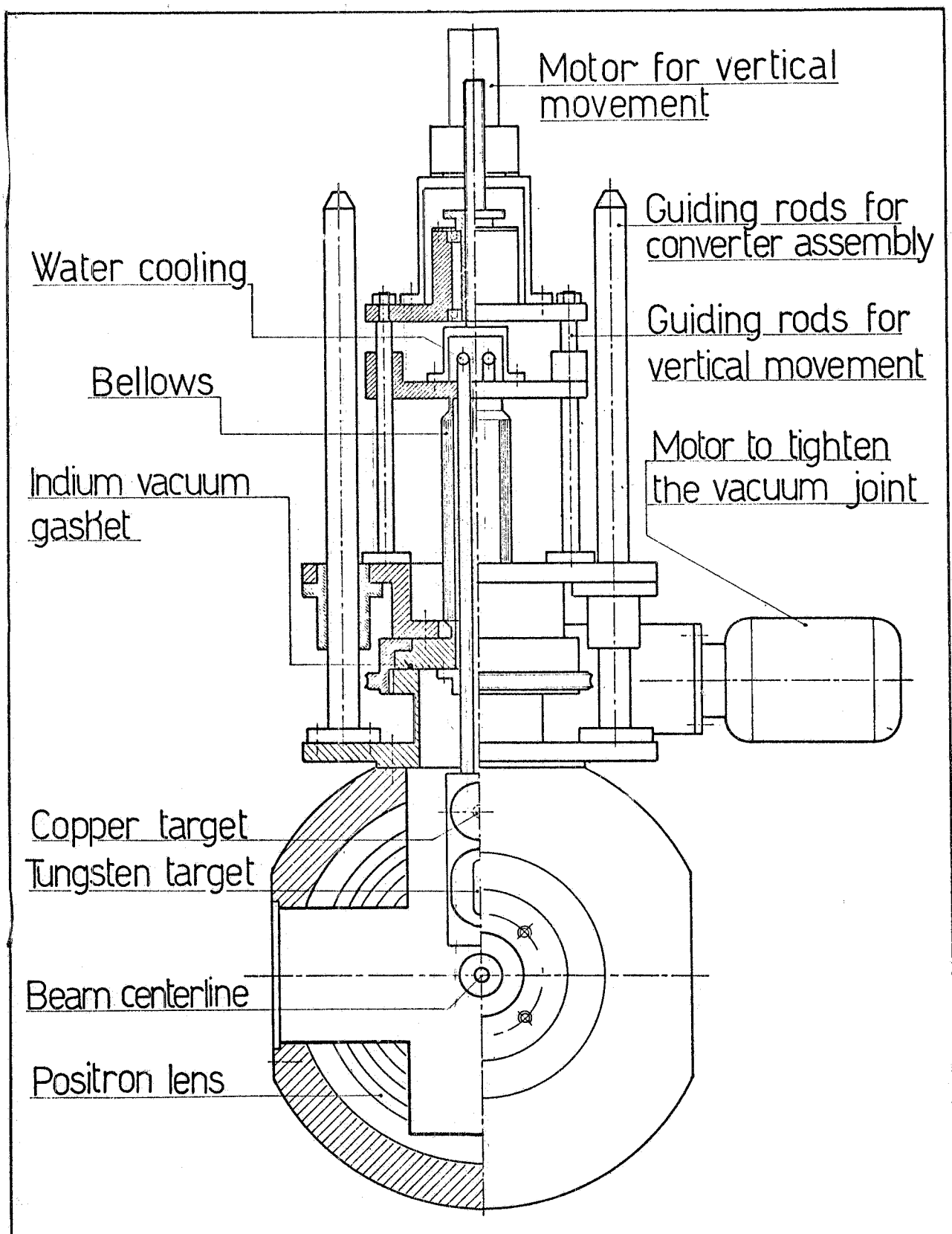


FIG. 3 - Positron converter layout.